Planta (2021) 253:125
https://doi.org/10.1007/s00425-021-03643-y

ORIGINAL ARTICLE

Highly degenerate plastomes in two hemiparasitic dwarf mistletoes: *Arceuthobium chinense* and *A. pini* (Viscaceae)

Xiaorong Guo[1,2] · Guangfei Zhang[1,2] · Linyuan Fan[3] · Changkun Liu[4] · Yunheng Ji[4,5]

Received: 5 January 2021 / Accepted: 19 May 2021 / Published online: 24 May 2021

Abstract

Main conclusion **The leafless and endophytic habitat may significantly relax the selection pressure on photosynthesis, and plastid transcription and translation, causing the loss/pseudogenization of several essential plastid-encoding genes in dwarf mistletoes.**

Abstract Dwarf mistletoes (*Arceuthobium* spp., Viscaceae) are the most destructive plant parasites to numerous conifer species worldwide. In this study, the plastid genomes (plastomes) of *Arceuthobium chinense* Lecomte and *A. pini* Hawksworth and Wiens were sequenced and characterized. Although dwarf mistletoes are hemiparasites capable of photosynthesis, their plastomes were highly degenerated, as indicated by the smallest plastome size, the lowest GC content, and relatively very few intact genes among the Santalales hemiparasites. Unexpectedly, several essential housekeeping genes (*rpoA*, *rpoB*, *rpoC1*, and *rpoC2*) and some core photosynthetic genes (*psbZ* and *petL*), as well as the *rpl33* gene, that is indispensable for plants under stress conditions, were deleted or pseudogenized in the *Arceuthobium* plastomes. Our data suggest that the leafless and endophytic habit, which heavily relies on the coniferous hosts for nutrients and carbon requirement, may largely relax the selection pressure on photosynthesis, as well as plastid transcription and translation, thus resulting in the loss/pseudogenization of such essential plastid-encoding genes in dwarf mistletoes. Therefore, the higher level of plastome degradation in *Arceuthobium* species than other Santalales hemiparasites is likely correlated with the evolution of leafless and endophytic habit. A higher degree of plastome degradation in *Arceuthobium*. These findings provide new insights into the plastome degeneration associated with parasitism in Santalales and deepen our understanding of the biology of dwarf mistletoes.

Keywords Endophytic habit · Reductive evolution · *Rpo* genes · *rpl33* · Gene loss · Santalales

Introduction

The sandalwood order Santalales, with 20 families and approximately 160 genera and 2200 species (Der and Nickrent 2008; Nickrent et al. 2010, 2019; Su et al. 2015), harbors the richest diversity of parasites within the plant kingdom, including lifestyles from autotrophy to hemiparasitism and holoparasitism (Nickrent 1997, 2002; Der and

Communicated by Anastasios Melis.

Xiaorong Guo and Guangfei Zhang contributed equally to this study.

✉ Yunheng Ji
jiyh@mail.kib.ac.cn

[1] Institute of Ecology and Geobotany, Yunnan University, Kunming, Yunnan, China

[2] School of Ecology and Environmental Science, Yunnan University, Kunming, Yunnan, China

[3] Yunnan General Administration of Forestry Seeds and Seedlings, Kunming, Yunnan, China

[4] CAS Key Laboratory for Plant Diversity and Biogeography of East Asia, Kunming Institute of Botany, Chinese Academy of Sciences, Kunming, Yunnan, China

[5] Yunnan Key Laboratory for Integrative Conservation of Plant Species with Extremely Small Population, Kunming Institute of Botany, Chinese Academy of Sciences, Kunming, Yunnan, China

Nickrent 2008; Su et al. 2015). *Arceuthobium* (the dwarf mistletoes), which is found in both the Old and New worlds (Frank et al. 1996), is a genus belonging to the Santalales family Viscaceae. According to the most recent taxonomic revision (Frank et al. 1996; Nickrent et al 2010), the genus comprises approximately 42 species of stem parasites that are capable of photosynthesis (Hull and Leonard 1964a, b; Leonard and Hull 1965; Mathiasen et al. 2008). *Arceuthobium* is the most host-specialized taxon in Santalales, and the species of the genus exclusively parasitize members of Pinaceae and Cupressaceae (Frank et al. 1996). The lifecyle mistletoes is also particularly unusual among the Santalales hemiparasites. Compared with close relatives, the leaves of dwarf mistletoes are extremely reduced and their body sizes are only several centimeters in height (Frank et al. 1996). In addition, *Arceuthobium* species do not produce shoots immediately after seed germination, but develop a highly developed haustorial system that thoroughly permeates inside the branches of their coniferous hosts (endophytic system); after 2–6 years, aerial shoots arise from the endophytic system (Parmeter et al. 1959; Parmeter and Scharpf 1963; Tong and Ren 1980; Frank et al. 1996; Mathiasen et al. 2008). The extensive endophytic system of dwarf mistletoes enables them to absorb nutrition and water from host plants with significantly higher efficiency than other Santalales hemiparasites (Baranyay et al. 1971; Tocher et al. 1984; Alosi and Calvin 1985; Kirkpatrick 1989; Singh and Carew 1989). This makes *Arceuthobium* species relatively unique among mistletoes. The leafless and endophytic habit indicates a greater reliance on host plants for nutrients. It is estimated that dwarf mistletoes absorb as much as 80% of their carbon requirement from their hosts (Frank et al. 1996; Parks and Flanagan 2001; Mathiasen et al. 2008). Severe infection by dwarf mistletoes always leads to significant growth declines and premature mortality in their coniferous hosts (Mathiasen et al. 2008). Therefore, epidemics of dwarf mistletoe infection always significantly damage coniferous forests worldwide (Frank et al. 1996).

In green plants, chloroplasts are organelles that conduct photosynthesis and the biosynthesis of starch, fatty acids, pigments, and amino acids (Palmer 1985; Neuhaus and Emes 2000; Daniel et al. 2016). In most angiosperms, plastid genomes (plastomes) are maternally inherited and highly conserved in size, structure, gene content, and organization (Daniel et al. 2016). The structure of a typical angiosperm plastome is circular and quadripartite and consists of a large single copy region (LSC), a small single copy region (SSC), and a pair of inverted repeats (IRs) (Wicke et al. 2011a,b). Nevertheless, the lifestyle transition from autotrophy to heterotrophy in angiosperms always leads to massive modification of plastomes, involving size reduction, structural arrangements, and loss or pseudogenization of plastid genes, among other changes (Neuhaus and Emes 2000; Wicke and Naumann 2018). As a result, the plastome features of parasitic plants largely differ from those of their autotrophic relatives (Krause 2008; Wicke et al. 2013, 2016; Petersen et al. 2015; Frailey et al. 2018; Schneider et al. 2018; Shin and Lee 2018; Wicke and Naumann 2018; Guo et al. 2020, 2021). To date, the complete plastome of several Santalales parasites has been sequenced, providing valuable data to disentangle the evolutionary trajectory of plastome reduction associated with parasitism (Petersen et al. 2015; Su and Hu 2016; Li et al. 2017; Yang et al. 2017; Liu et al. 2018; Shin and Lee 2018; Zhu et al. 2018; Guo and Ruan 2019a, b; Jiang et al. 2019; Guo et al. 2019, 2020, 2021; Chen et al. 2020a, b).

Characterization of the complete plastomes of dwarf mistletoes will deepen our understanding of their biology, and because of their significant threats to numerous conifer species worldwide, genomic resources will be conducive to further studies on dwarf mistletoes involving phylogeny, population genetics, and interactions between dwarf mistletoes and their host plants. To date, the complete plastome of only one species, *Arceuthobium sichuanense* (HS Kiu) Hawksworth & Wiens, has been sequenced (Chen et al. 2020a, b). This represents merely a small fraction of the species diversity in the genus. Thus, the extent to which the plastomes of dwarf mistletoes are degraded and whether their leafless and endophytic habit is correlated with a higher level of plastome reduction than other Santalales hemiparasites remains undetermined.

Here, the complete plastomes of *A. chinense* and *A. pini* were sequenced and assembled using the genome skimming approach (Straub et al. 2012). The study was based on a comparative and phylogenetic framework, and the main objectives were as follows: (1) To characterize the genome size, structure, and gene content of the plastomes, and (2) To elucidate whether the leafless and endophytic habit of dwarf mistletoes leads to a higher level of plastome reduction than other Santalales hemiparasites.

Materials and methods

Plastome sequencing, assembly, and annotation

Plant tissues of *A. chinense* and *A. pini* collected from the wild were dried with silica gel, and voucher specimens (Table 1) were deposited in the herbarium of the Kunming Institute of Botany, Chinese Academy of Sciences (KUN), Kunming, China. Total genomic DNA was extracted from ~ 50 mg of silica gel-dried leaves using cetyltrimethylammonium ammonium bromide following the protocol of Doyle and Doyle (1987). Purified DNA was fragmented with Covaris S2 to an average length of ~ 350 bp, followed by ligation of adaptors for library amplification according to the

Table 1 Voucher information of the two *Arceuthobium* species observed in this study and the summary of shotgun sequencing and plastome assembly

	Arceuthobium chinense	*A. pini*
Locality	Huafoshan Mountain, Mouding, Yunnan, China	Benzilan, Deqin, Yunnan, China
Host plant	*Keteleeria evelyniana*	*Pinus densata*
Voucher specimen	Zhang GF 009	Su WH 002
No. of clean reads	19,807,964	19,297,440
No. of mapped reads	595,837	323,977
Plastome size (bp)	116,594	115,862
Coverage (×)	822.262	447.011
GenBank accessions	MT635188	MT635189

manufacturer's guidelines (Illumina, San Diego, CA, USA). Paired-end shotgun sequencing (2 × 150 bp) was performed on the Illumina HiSeq 2500 platform at Personal Biotechnology (Shanghai, China) to generate approximately 4.5 G raw data for each sample.

A FASTX–Toolkit v.0.0.13 (http://hannonlab.cshl.edu/fastx_toolkit) was used to remove adaptors and reads with ambiguous bases from the raw Illumina data. The clean reads were de novo assembled using the software NOVOPlasty v.2.7.0 (Dierckxsens et al. 2017), with the *k-mer* size set at 31. The large subunit of the RuBisCO gene (*rbcL*) of *A. azoricum* (HM849787) was used as the seed for the iterative extension of contigs to recover the complete plastome of each species. The newly generated plastomes were annotated using the Dual Organellar Genome Annotator database (Wyman et al. 2004). The annotation of protein-coding genes was confirmed using a BLAST search against the NCBI protein database. The protein-coding genes with one or more frameshift mutations or premature stop codons were annotated as pseudogenes. Genes putatively annotated as transfer RNA (tRNA) were further verified by tRNAscan-SE v.1.21 (Schattner et al. 2005) with default parameters.

Comparative and phylogenetic analyses

Previously published plastomes of Santalales (Petersen et al. 2015; Su and Hu 2016; Li et al. 2017; Yang et al. 2017; Liu et al. 2018; Shin and Lee 2018; Zhu et al. 2018; Guo and Ruan 2019a, b; Jiang et al. 2019; Guo et al. 2019, 2020, 2021; Chen et al. 2020a, b) were downloaded from the NCBI GenBank for comparative and phylogenetic analyses (Table S1). The structure and gene content of the Santalales plastomes were compared using Geneious v10.2 (Kearse et al. 2012). Any putative gene deletions detected in the newly generated dwarf mistletoe plastomes were further verified by extracting intact sequences of the corresponding genes from the plastome of *Erythropalum scandens* Blume (Erythropalaceae, Santalales), the autotrophic relative of dwarf mistletoes, and then performing local BLAST searches against the Illumina reads of each sample. Following this, all *Arceuthobium* plastomes were pairwise-aligned using mVISTA (Mayor et al. 2000) to investigate sequence divergence.

Both standard maximum likelihood (ML) and Bayesian inference (BI) approaches were used to infer the phylogenetic relationships between *Arceuthobium* and related taxa. Based on the interfamilial relationships of Santalales recovered in previous studies (Der and Nickrent 2008; Nickrent et al. 2010, 2019; Su et al. 2015; Chen et al. 2020a, b; Guo et al. 2020, 2021), *E. scandens* was selected as the outgroup to root the phylogenetic trees. Forty-six plastid protein-coding genes commonly shared by the taxa were used in the phylogenetic reconstruction. These genes were separately aligned using MAFFT v.7.450 (Katoh and Standley 2013) and then integrated into a data set using Geneious v10.2 (Kearse et al. 2012).

The ML analyses were performed using RAxML-HPC BlackBox v8.1.24 (Stamatakis et al. 2008), using the sequence substitution model (GTRGAMMAI). The phylogenetic tree was inferred by conducting ten independent ML searches with 1000 replicates of standard bootstrapping (BS). The BI analyses were performed using MRBAYES v.3.1.2, (Ronquist and Huelsenbeck 2003). Runs of Markov chain Monte Carlo simulations were initiated with a random tree for one million generations, with trees sampled every 100 generations. Trees that resulted from the first 25% of generations were discarded as "burn-in" The posterior probability values (PP) were computed based on the remaining trees.

Results

Plastome features of newly sequenced *Arceuthobium* species

Illumina paired-end sequencing yielded over 19 million clean reads for each species; the mean depth of the plastome sequencing was 822 × for *A. chinense* and 447 × for *A. pini* (Table 1). The assembled plastomes of *A. chinense* and *A. pini* were 116,594 bp and 115,862 bp in size, respectively. They possessed a typical quadripartite structure (Fig. 1), consisting of a pair of IRs (21,333 and 21,303 bp, respectively), an LSC (66,071 and 65,229 bp, respectively), and an SSC (7857 and 8027 bp, respectively). In comparison with other Santalales plastomes (Table 2). The *Arceuthobium* species had the lowest GC content (33.7–34.9%), which was unevenly distributed in the LSC, SSC, and IRs. The highest GC content was in the IR regions (42.1–42.3%), followed by the LSC (29.7–30.1%). The lowest GC content was observed

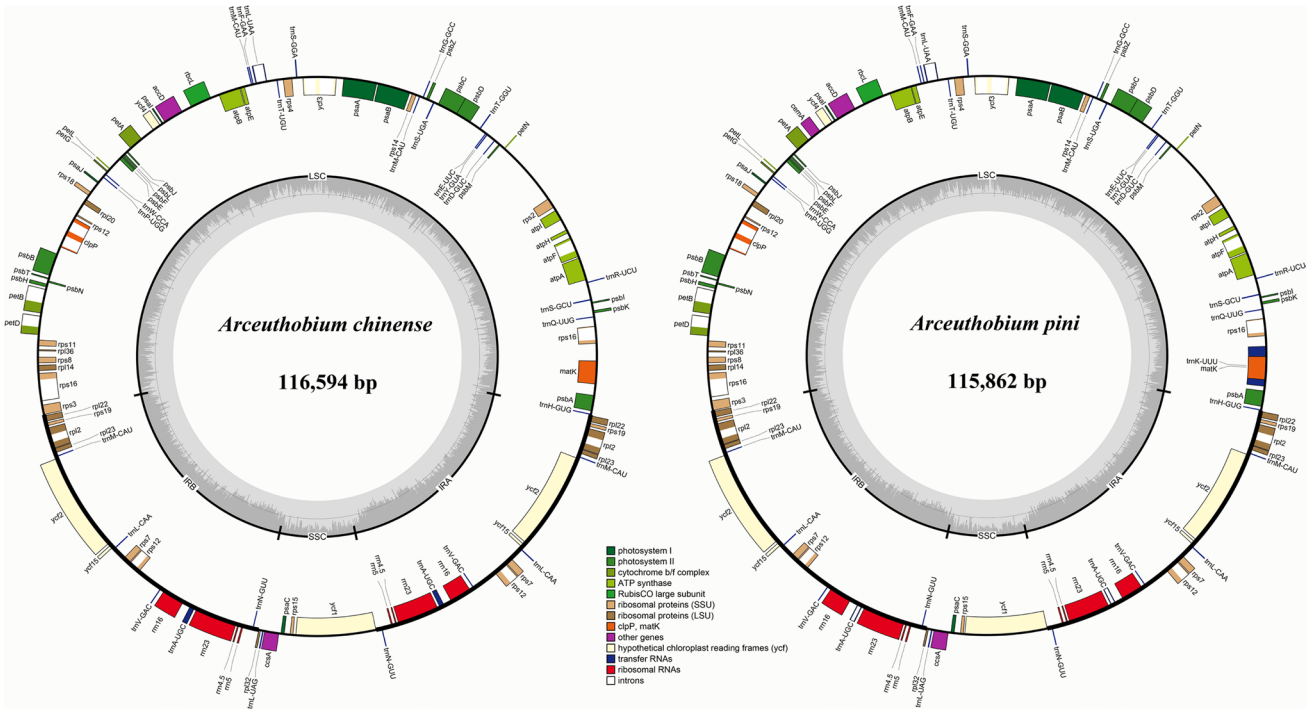

Fig. 1 Plastome map of *Arceuthobium chinense* and *A. pini*

in the SSC (21.5–26.4%). The plastome-wide comparative analysis using the mVISTA program detected 2510 sequence variations among the 120,242 alignment sites, accounting for 2.087% of the divergence proportion among *A. chinense*, *A. pini*, and *A. sichuanense* (Fig. 2).

The plastomes of *A. chinense* and *A. pini* contained 86 and 88 intact genes, respectively (Table 3). In contrast to the non-parasitic plant *E. scandens*, all 11 NAD(P)H-dehydrogenase (NDH) complex genes (*ndhA*, *B*, *C*, *D*, *E*, *F*, *G*, *H*, *I*, *J*, and *K*), four RNA polymerase genes (*rpoA*, *rpoB*, *rpoC1*, and *rpoC2*), a ribosomal protein-coding gene (*rpl33*), the *infA* gene, as well as six tRNA genes (*trnC-GCA*, *trnG-UCC* , *trnH-GUG*, *trnI-GAU*, *trnR-ACG*, and *trnV-UAC*) were deleted from the plastomes. Two photosynthesis-related genes (*petL* and *psbZ*) were identified as pseudogenes in both species because of the occurrence of premature stop codons. Moreover, an additional loss of *cemA* and *trnK-UUU* was detected in *A. chinense*. As a result of gene loss and pseudogenization, 59 and 60 protein-encoding genes, respectively, and four ribosomal RNA genes, as well as 23 and 24 tRNAs, respectively, were retained in the *A. chinense* and *A. pini* plastomes.

Comparison of plastome structure and gene content

The junctions of IR/LSC and IR/SSC were highly variable in the plastomes of Santalales hemiparasites due to the expansion/contraction of IRs (Fig. 3). Although the examined Santalales hemiparasites had divergent gene content in their plastomes (Fig. 4), the loss or pseudogenization of plastid *ndh* genes were commonly shared. Of these taxa, the plastomes of Amphorogynaceae, Santalaceae, Schoepfiaceae, and Ximeniaceae encoded the highest number of intact plastid genes, with a total of 101 to 102, including 66–68 protein-coding genes, 29–30 tRNA genes, and four rRNA genes. Comparatively, the lowest number of intact genes was observed in *Arceuthobium*, which possessed 54–60 protein-coding genes, 23–24 tRNA genes, and four rRNA genes. In addition, pseudogenization or loss of *infA* was found in Amphorogynaceae, Cervantesiaceae, Loranthaceae, Opiliaceae, Santalaceae, and Viscaceae. The deletion of *trnV-UAC* genes was shared by species of Loranthaceae, Schoepfiaceae, and Viscaceae. Further loss of *trnG-UCC* was detected in Loranthaceae and Viscaceae. The losses of *rpl32*, *rps15*, *rps16*, *trnG-UCC*, and *trnK-UUU* occurred in Loranthaceae. The pseudogenization of some essential photosynthetic genes (*psbZ*, *petL*, and *ccsA*) was identified in Viscaceae, whereas the deletion of RNA polymerase genes (*rpoA*, *rpoB*, *rpoC1*, and *rpoC2*) only occurred in *Arceuthobium.*

Phylogenetic analyses

The ML and BI analyses produced identical tree topologies (Fig. 5). Ximeniaceae (root hemiparasitism) was resolved as an early diverged branch (BS = 100%,

Table 2 Comparison of size and GC content (GC%) of complete plastomes, LSC, IR, and SSC regions among Santalales plastomes

Species*	Plastome		LSC		IR		SSC	
	Size (bp)	GC (%)	Size (bp)	GC (%)	Size (bp)	GC (%)	Size (bp)	GC (%)
Arceuthobium sichuanense	107,526	34.9	65,171	30.1	21,045	42.3	265	26.4
Arceuthobium pinii	115,862	33.9	65,229	30.0	21,303	42.1	8027	21.5
Arceuthobium chinense	116,594	33.7	66,071	29.7	21,333	42.1	7857	21.6
Schoepfia jasminodora	118,743	38.1	84,168	36.1	12,406	47.9	9763	30.7
Taxillus delavayi	119,941	37.1	70,281	34.7	21,859	42.5	5942	26.9
Schoepfia fragrans	120,188	38.1	85,643	36.1	12,381	47.9	9783	30.6
Taxillus chinensis	121,363	37.3	70,357	34.7	22,462	43.0	6082	26.2
Taxillus nigrans	121,419	37.4	70,181	34.8	22,569	43.0	6100	26.2
Taxillus vestitus	122,200	37.3	70,250	34.8	22,923	42.8	6104	26.2
Taxillus thibetensis	122,286	37.2	70,018	34.5	23,074	42.7	6120	26.0
Dendrophthoe pentandra	122,451	36.3	72,451	33.6	22,118	42.2	5764	25.0
Taxillus sutchuenensis	122,562	37.3	70,630	34.7	22,915	42.8	6102	26.2
Loranthus tanakae	123,397	36.9	69,522	34.8	23,076	42.2	7723	24.4
Tolypanthus maclurei	123,581	36.8	72,952	34.3	22,185	42.4	6259	26.0
Helixanthera parasitica	124,881	36.5	73,043	33.8	22,752	42.3	6334	25.5
Viscum crassulae	126,064	36.4	73,226	33.6	22,105	43.4	8628	24.0
Macrosolen tricolor	126,617	37.6	71,893	35.2	24,702	42.4	5320	25.8
Macrosolen sp.	128,459	37.3	73,347	34.8	22,960	43.3	9192	27.3
Viscum liquidambaricolum	128,601	36.1	73,831	33.1	23,041	43.2	8688	23.7
Viscum coloratum	128,746	36.3	73,686	33.4	23,215	43.1	8630	24.3
Viscum album	128,921	36.4	73,893	33.5	23,198	43.2	8632	24.8
Viscum ovalifolium	129,465	36.1	74,348	33.2	23,203	43.1	8711	24.2
Pyrularia sinensis	130,015	37.3	83,917	35.0	19,316	40.7	7466	46.3
Viscum yunnanens	130,721	35.8	75,844	32.8	22,894	43.3	9089	22.6
Viscum minimum	131,016	36.2	75,814	33.3	23,094	43.2	9014	24.2
Pyrularia edulis	132,808	38.3	74,811	36.1	24,548	42.8	8901	31.2
Phacellaria glomerata	138,684	37.9	79,937	35.6	24,080	43.6	10,587	29.6
Phacellaria compressa	138,903	37.9	80,099	35.6	24,104	43.6	10,596	29.5
Dendrotrophe varians	140,666	37.8	81,684	35.5	24,056	43.7	10,870	29.7
Santalum album	144,101	38.0	83,802	35.9	24,511	43.1	11,277	31.4
Santalum boninense	144,263	38.0	83,912	35.9	24,501	43.1	11,349	31.6
Osyris alba	147,253	37.7	84,601	35.6	24,340	43.1	13,972	31.2
Champereia manillana	147,461	37.4	83,505	35.3	28,075	41.9	7806	27.9
Osyris wightiana	147,544	37.6	84,569	35.5	24,447	43.0	14,081	31.1
Erythropalum scandens	156,154	38.0	84,799	36.2	26,394	42.8	18,567	32.3
Ximenia americana	156,834	36.8	87,816	34.4	32,691	40.4	3636	27.5
Malania oleifera	158,163	36.7	87,212	34.4	35,256	39.6	439	25.7

**The species are arranged from the smallest to the largest by overall plastome size*

PP = 1.00), and the remaining Santalales hemiparasites formed two well-supported clades (BS = 100%, PP = 1.00). Within the first clade, the sister relationship between Schoepfiaceae (root hemiparasitism) and Loranthaceae (stem hemiparasitism) received high branch support (BS = 100%, PP = 1.00). Within the second clade, the successive divergence of the families Opiliaceae (root hemiparasitism), Cervantesiaceae (root hemiparasitism), Santalaceae (root hemiparasitism), Amphorogynaceae (stem hemiparasitism), and Viscaceae (stem hemiparasitism) were recovered with high statistical support (BS = 100%, PP = 1.00).

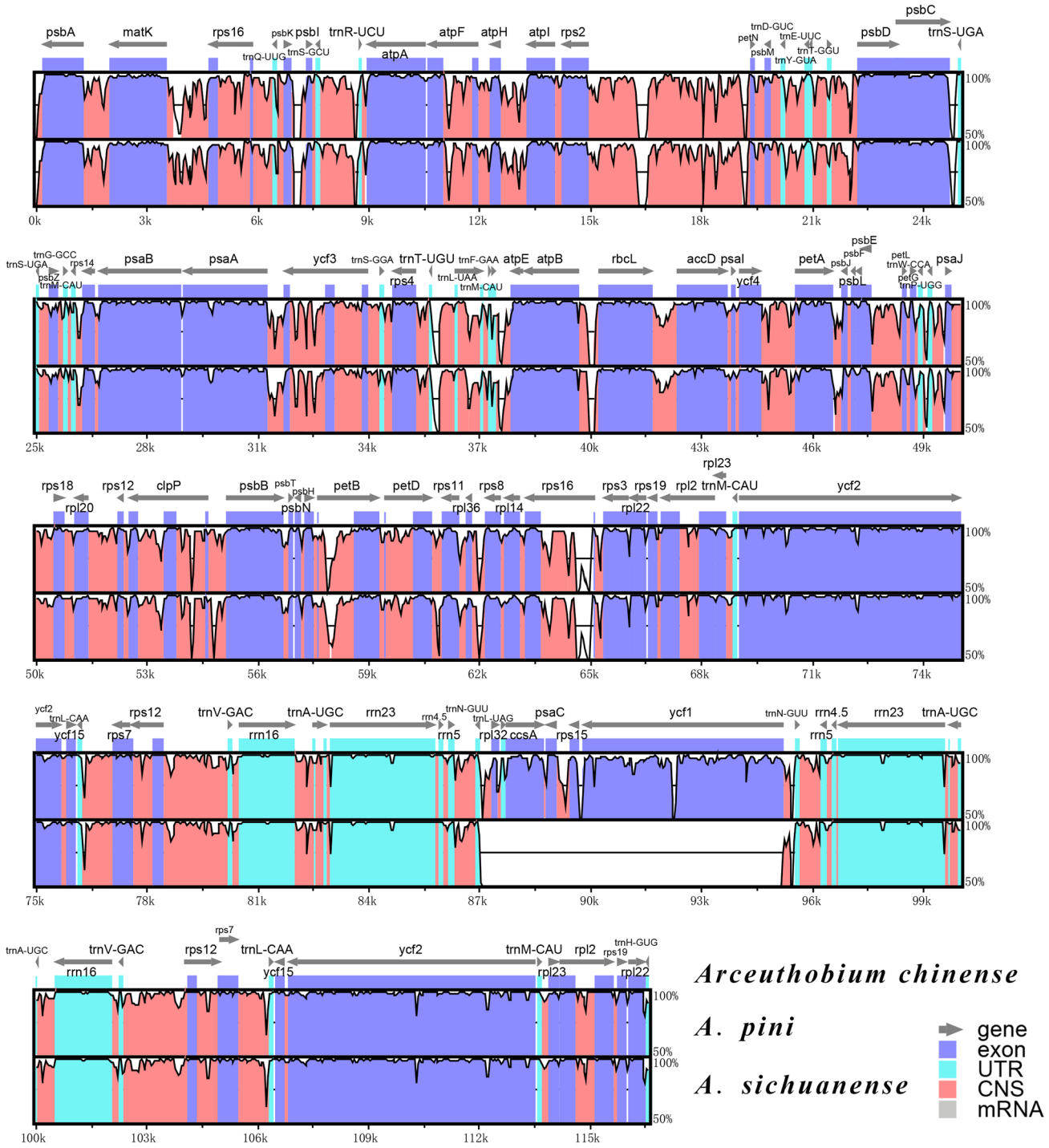

Fig. 2 Alignment of three *Arceuthobium* plastomes using mVISTA, showing the percentages of sequence identity (*y*-axis)

Discussion

Plastome reduction in Santalales hemiparasites

The lifestyle transition from autotrophy to heterotrophy always leads to prevalent gene losses from the plastomes of parasitic plants (Neuhaus and Emes 2000; Wicke et al. 2013, 2016; Wicke and Naumann 2018). A great diversity of plastome sizes, GC content, and the number of functional (intact) genes were observed in Santalales hemiparasites (Table 2), suggesting that their plastomes undergo significant modifications associated with the evolution of

Table 3 Comparison of plastome gene content between Santalales hemiparasites and the autotropic relative *Erythropalum scandens*

Species	Total plastid genes	Potentially functional genes	Functional protein-encoding genes	tRNA	rRNA	Deleted genes	Pseudogenes
Erythropalum scandens	113	113	79	30	4	0	0
Osyris alba	110	101	67	30	4	3	9
Osyris wightiana	110	101	67	30	4	3	9
Santalum album	108	101	67	30	4	5	7
Santalum boninense	108	101	67	30	4	5	7
Champereia manillana	105	100	66	30	4	8	5
Dendrotrophe varians	105	101	67	30	4	8	4
Phacellaria compressa	103	101	67	30	4	10	2
Phacellaria glomerata	103	101	67	30	4	10	2
Ximenia americana	103	102	68	30	4	10	1
Malania oleifera	102	102	68	30	4	11	0
Pyrularia edulis	102	100	67	29	4	11	2
Schoepfia fragrans	101	101	68	29	4	12	0
Schoepfia jasminodora	101	101	68	29	4	12	0
Viscum minimum	101	99	66	29	4	12	2
Viscum yunnanens	101	97	64	29	4	12	4
Viscum album	100	97	65	28	4	13	3
Viscum coloratum	100	96	64	28	4	13	4
Viscum liquidambaricolum	100	97	65	28	4	13	3
Viscum ovalifolium	100	97	65	28	4	13	3
Viscum crassulae	99	98	66	28	4	14	1
Pyrularia sinensis	97	94	62	28	4	16	3
Macrosolen sp.	96	94	63	27	4	17	2
Macrosolen tricolor	96	95	64	27	4	17	1
Taxillus sutchuenensis	96	94	63	27	4	17	2
Taxillus chinensis	95	94	63	27	4	18	1
Taxillus thibetensis	95	94	63	27	4	18	1
Taxillus vestitus	95	95	64	27	4	18	0
Dendrophthoe pentandra	94	92	63	25	4	19	2
Loranthus tanakae	94	90	61	25	4	19	4
Taxillus nigrans	94	92	62	26	4	19	2
Tolypanthus maclurei	94	93	64	25	4	19	1
Helixanthera parasitica	93	92	63	25	4	20	1
Taxillus delavayi	93	93	64	25	4	20	0
Arceuthobium pini	90	88	60	24	4	23	2
Arceuthobium chinense	88	86	59	23	4	25	2
Arceuthobium sichuanense	84	81	54	23	4	29	3

parasitism (Wicke and Naumann 2018). Compared with the autotrophic relative, *E. scandens*, the plastid GC content was lower not only in *Arceuthobium* but also in other Santalales hemiparasites (Table 2). Here, empirical evidence is provided to justify the idea that loss/pseudogenization of plastid genes from parasitic plants is accompanied by a reduction in the GC content in their plastomes (Wicke and Naumann 2018). Notably, diverse IR shifts were observed in the plastomes of Santalales hemiparasites (Fig. 3), which supports the hypothesis that decreasing GC content may trigger significant IR expansion/contraction in the plastomes of parasitic species (Wicke et al. 2013, 2016).

A typical angiosperm plastome contains 113 unique genes, including 79 protein-coding genes, 30 rRNA genes, and four ribosomal RNA genes (Wicke et al. 2011a,b). In the examined Santalales taxa, only the autotrophic *E. scandens* plastome contained relatively intact gene content. Because of gene loss and pseudogenization, only 86 and 88 functional genes were retained in the plastomes of *A. chinense* and *A. pini*, respectively. Similar levels of gene loss and

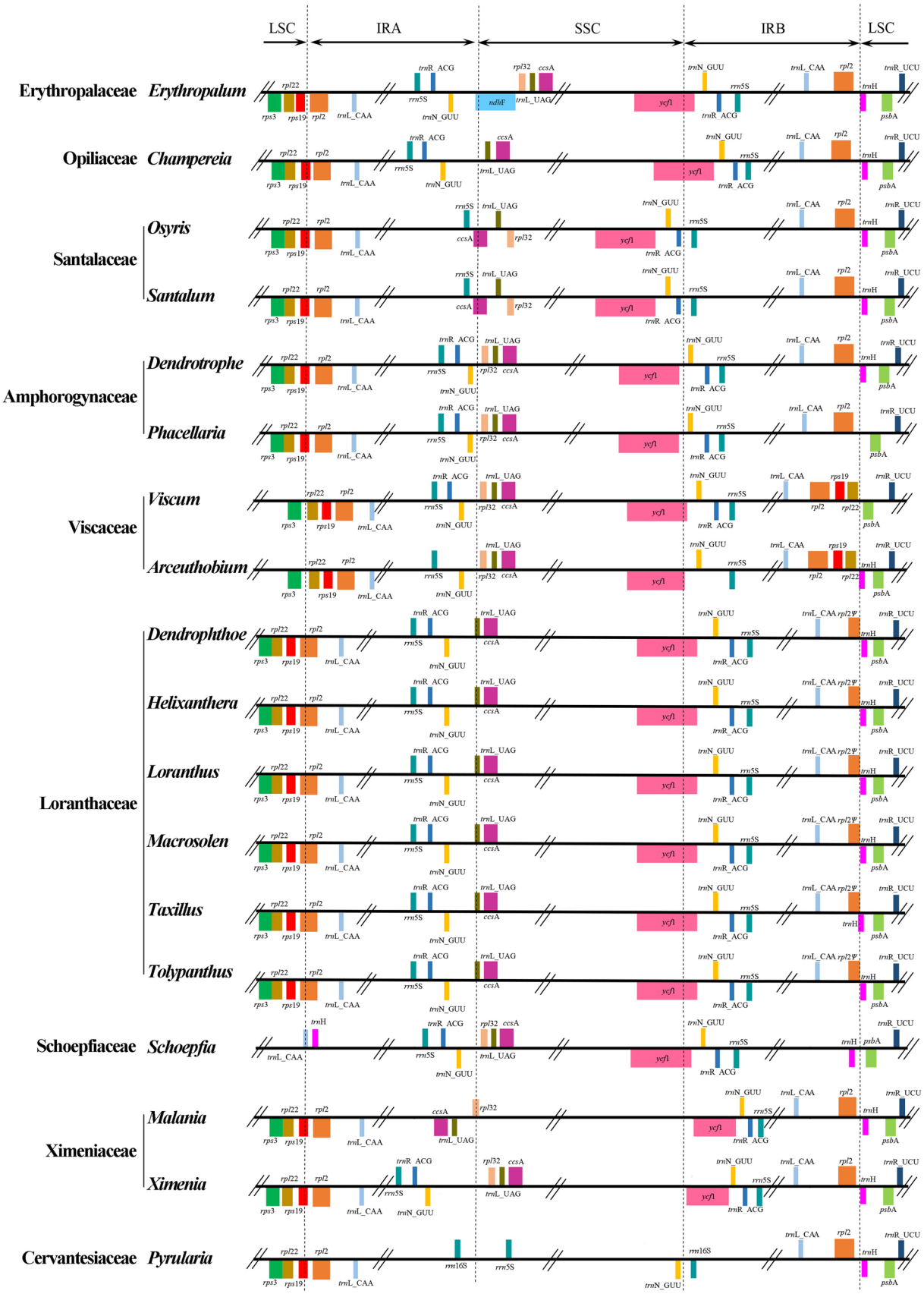
LSC
IRA
SSC
IRB
LSC
Erythropalaceae
Erythropalum
Opiliaceae
Champereia
Santalaceae
Osyris
Santalum
Amphorogynaceae
Dendrotrophe
Phacellaria
Viscaceae
Viscum
Arceuthobium
Loranthaceae
Dendrophthoe
Helixanthera
Loranthus
Macrosolen
Taxillus
Tolypanthus
Schoepfiaceae
Schoepfia
Ximeniaceae
Malania
Ximenia
Cervantesiaceae
Pyrularia

◂**Fig. 3** Boundaries of inverted repeats (IRA and IRB), large single copy (LSC), and small single copy (SSC) regions are compared at genus-level to show the dynamics of IR expansion/contraction among Santalales plastomes

pseudogenization were also observed in the congeneric species, *A. sichuanense* (Fig. 4; Table 3). This decrease in functional genes suggests that the relatively small plastome size of *Arceuthobium* species compared with that of *E. scandens* can be partially attributed to heterotrophy-associated gene losses. Previous studies have indicated that the losses of some plastid genes resulted in varying degrees of plastome downsizing in Santalales hemiparasites (Petersen et al. 2015; Shin and Lee 2018; Chen et al. 2020a, b; Guo et al. 2020, 2021).

The loss/pseudogenization of plastid *ndh* genes is commonly observed in parasitic plants, which is regarded as an early response of plastomes in the evolution of heterotrophic lifestyles (Wicke and Naumann 2018). The observation that all 11 *ndh* (*A* to *K*) genes were either deleted or pseudogenized in the examined Santalales hemiparasites (Fig. 4) further confirms the assumption that the NDH pathway is not indispensable in parasitic plants that retain photosynthetic capacity (Maier et al. 2007; Wicke and Naumann 2018). Remarkably, the loss/pseudogenization of these plastid–encoded *ndh* genes has also been observed in a variety of photoautotrophic plants, including gymnosperms (e.g., Wakasugi 1994; McCoy et al. 2008; Wu et al. 2009; Ni et al. 2017), monocots (e.g., Peredo et al. 2013; Chang et al. 2006; Lin et al. 2015, 2017), early diverging eudicots (e.g., Sun et al. 2016, 2017), and core eudicots (e.g., Sanderson et al. 2015; Blazier et al. 2011; Morais et al. 2021). Given the independent loss of this pathway in many plant lineages, it is proposed that the plastid *ndh* genes may have been selected against in photoautotrophic angiosperms (Frailey et al. 2018). In addition, Lin et al. (2017) proposed that the loss of the plastid NDH pathway in photoautotrophic plants may increase the possibility of evolving a heterotrophic life history. Therefore, the reduction in the NDH pathway in the plastomes of the Santalales hemiparasites is more likely to be a trigger than an outcome of evolution to a parasitic lifestyle. On the other hand, the degradation of the NDH pathway always causes severe phenotypic and physiological effects in plants experiencing light, water, or heat stress (Horváth et al. 2000; Rumeau et al. 2007). Given that infections by *Arceuthobium* species pose major threats to coniferous forests worldwide (Tong and Ren 1980; You 1985; You and Tong 1987; Frank et al. 1996; Mathiasen et al. 2008), the eco-physiological consequences of the loss of plastid *ndh* genes in dwarf mistletoes (especially under stress conditions) need to be further investigated.

The *infA* gene is another commonly reduced gene in the plastomes of Santalales hemiparasites. This degradation occurs in all Santalales hemiparasites, except for Ximeniaceae and Schoepfiaceae. Although the loss or pseudogenization of *infA* is generally observed in the plastomes of many holoparasitic plants (Wicke et al. 2011a,b,2013,2016; Wicke and Naumann 2018), this mutation is quite rare in hemiparasites and has so far been identified in Santalales (Petersen et al. 2015; Li et al. 2017; Yang et al. 2017; Liu et al. 2018; Shin and Lee 2018; Zhu et al. 2018; Jiang et al. 2019; Chen et al. 2020a, b; Guo et al. 2020, 2021). Nevertheless, pseudogenization or deletion of the *infA* gene has been identified in a wide range of photoautotrophic angiosperms (Millen et al. 2001; Ahmed et al. 2012; Wicke and Naumann 2018). Therefore, the degradation of this gene in Santalales hemiparasites may not be associated with the evolution of the parasitic lifestyle. Although *infA* is an essential gene for the initiation of translation in organelles (Pel and Grivell 1994; Yu and Spremulli 1998), earlier studies suggest that it is one of the most mobile plastid genes in angiosperms, which is often transferred to and maintained in the nucleus (Millen et al. 2001; Ahmed et al. 2012). Similarly, the plastid *infA* gene of the above-mentioned Santalales hemiparasites may have been transferred to the nucleus.

In addition to the loss/pseudogenization of *ndh* loci and *infA*, the deletion of *rps15*, *rps16*, and *rpl32* was commonly found in Loranthaceae species. Similarly, losses of these plastid ribosomal protein-encoding genes have been observed in a wide spectrum of autotrophic angiosperms (e.g., Chumley 2006; Saski et al. 2005; Jansen et al. 2007; Wicke et al. 2011a,b; Sabir et al. 2014; Park et al. 2015; Schwarz et al. 2015; Morais et al. 2021), and a line of evidence suggests that their functions are replaced by nuclear-encoding ribosomal genes (Park et al. 2015). Given their essential roles in plastid translation (Fleischmann et al. 2011; Park et al. 2015), the plastid *rps15*, *rps16*, and *rpl32* genes of Loranthaceae plastomes may have been functionally transferred to the nucleus, and the deletion of these genes is unlikely to have resulted from the evolution of parasitism.

Arceuthobium and *Viscum* (Viscaceae) are hemiparasites that retain their photosynthetic capacity. Therefore, the loss/pseudogenization of several photosynthesis-associated genes, such as *psbZ*, *petL*, *cemA*, and *ccsA* (Fig. 4), in their plastomes was unexpected. *Arceuthobium* and *Viscum* represent the only two Santalales genera to date in which critical photosynthetic genes have been partially lost from the plastomes, although the deletion or pseudogenization of such genes is commonly observed in holoparasitic angiosperms (Funk et al. 2007; McNeal et al. 2007; Wicke et al. 2013, 2016; Wicke and Naumann 2018; Chen et al. 2020a, b; Liu et al. 2020). Wicke and Naumann (2018) proposed that the reduction in these essential photosynthesis genes most likely occurred around the transition from hemiparasitism to holoparasitism. Such plastome mutations in *Arceuthobium* and *Viscum* imply that (1) the reduction in these genes may have

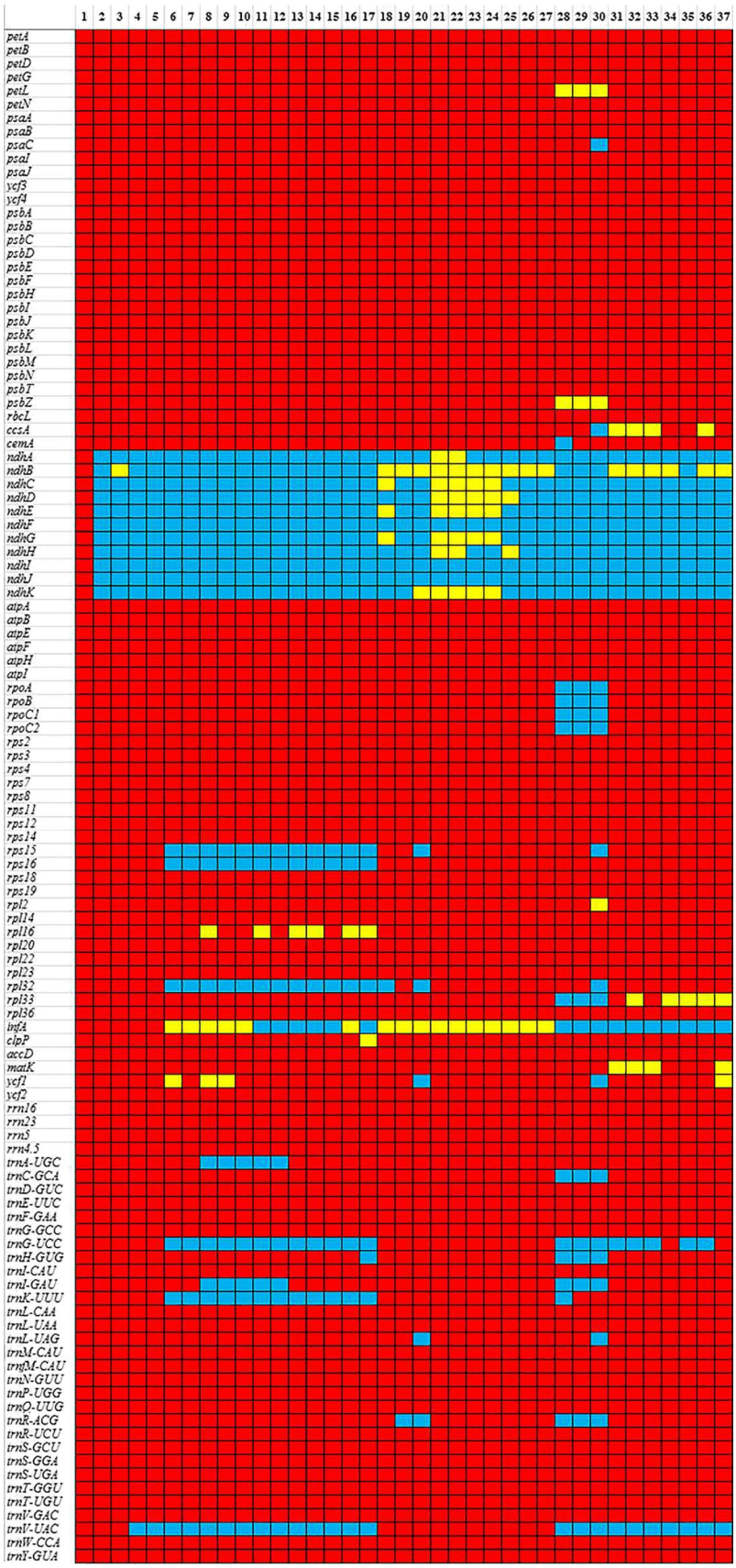

Fig. 4 Comparison of gene content among Santalales plastomes. 1: *Erythropalum scandens* (Erythropalaceae). 2: *Malania oleifera*; 3: *Ximenia americana* (Ximeniaceae); 4: *Schoepfia fragrans*; 5: *S. jasminodora* (Schoepfiaceae); 6: *Macrosolen sp.*; 7: *M. tricolor*; 8: *Loranthus tanakae*; 9: *Dendrophthoe pentandra*; 10: *Tolypanthus maclurei*; 11: *Helixanthera parasitica*; 12: *Taxillus delavayi*; 13: *T. thibetensis*; 14: *T. chinensis*; 15: *T. vestitus*; 16: *T. sutchuenensis*; 17: *T. nigrans* (Loranthaceae); 18: *Champereia manillana* (Opiliaceae); 19: *Pyrularia edulis*; 20: *P. sinensis* (Cervantesiaceae); 21: *Osyris alba*; 22: *O. wightiana*; 23: *Santalum album*; 24: *S. boninense*. (Santalaceae). 25: *Dendrotrophe varians*; 26: *Phacellaria compressa*; 27: *P. glomerate* (Amphorogynaceae). 28: *Arceuthobium chinense*; 29: *A. pini*; 30: *A. sichuanense*; 31: *Viscum album*; 32: *V. coloratum*; 33: *V. ovalifolium*; 34: *V. minimum*; 35: *V. crassulae*; 36: *V. liquidambaricolum*; 37: *V. yunnanense* (Viscaceae). Red squares: intact genes; yellow squares: pseudogenes; blue squares: deleted genes

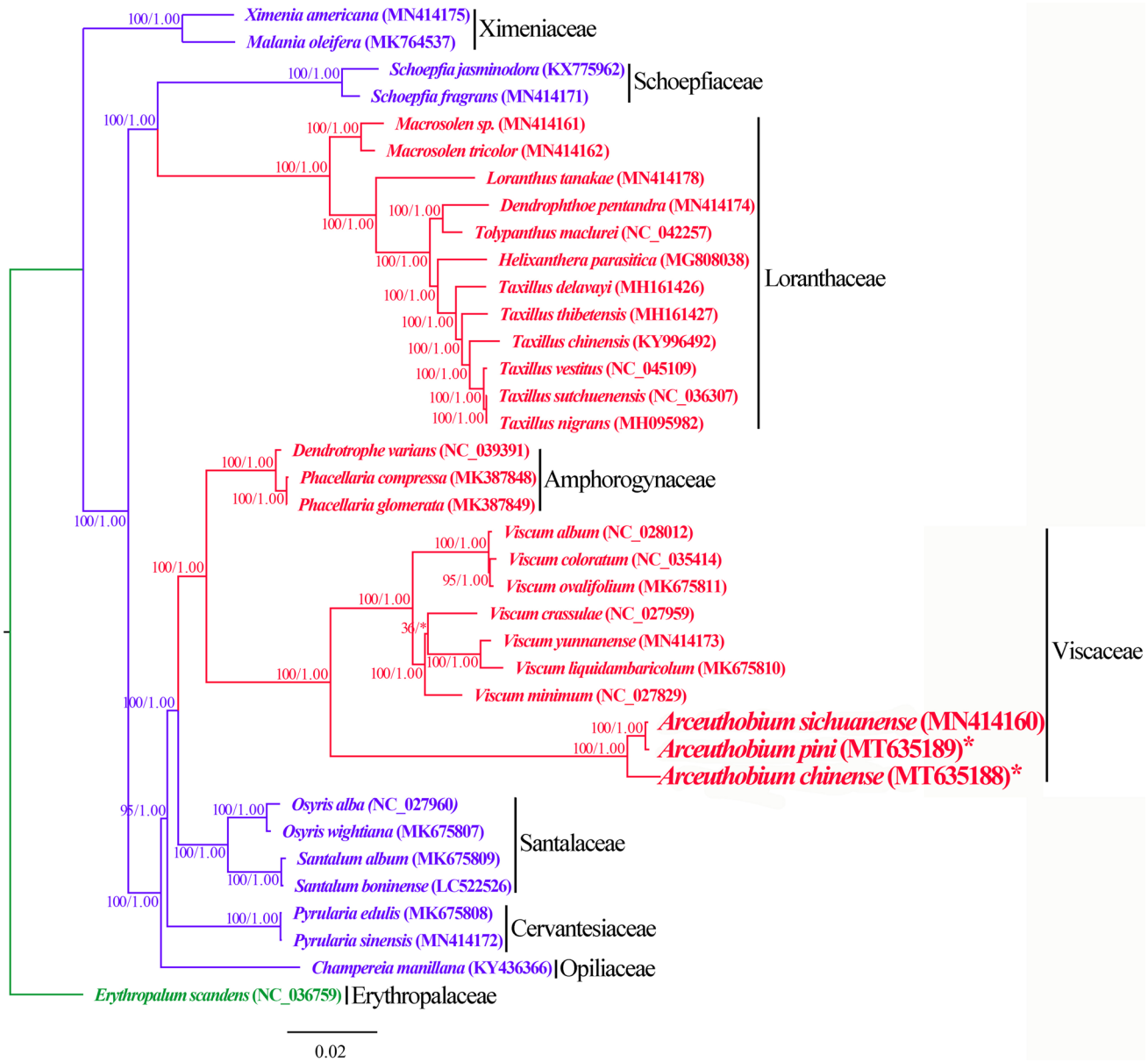

Fig. 5 Phylogeny of Santalales hemiparasites reconstructed by maximum-likelihood (ML) and Bayesian inference (BI) analyses of 46 protein-encoding genes. The numbers at each node are the maximum-likelihood bootstrap percentage (BS) and posterior probability (PP) values. Green lineages: autotrophy outgroup; blue lineages: root hemiparasites; red lineages: stem hemiparasites

been initiated in hemiparasites that still rely on photosynthesis, and that (2) the degeneration of photosynthetic capacity is a gradual process that may have been initiated at the hemiparasitic stage but is not likely completed until a holoparasitic lifestyle is achieved. Moreover, *Arceuthobium* and those *Viscum* species whose essential photosynthesis genes are partially deleted share the morphological similarity that their leaves are extremely degraded. As a result, they rely heavily on host plants for their carbon requirement (Frank et al. 1996; Parks and Flanagan 2001; Mathiasen et al. 2008), which may reduce the pressure on photosynthesis (Petersen et al. 2015; Wicke and Naumann 2018). Therefore, the loss/pseudogenization of such essential photosynthesis genes in *Arceuthobium* and some *Viscum* species is likely to be related to the evolution of the leafless habit.

In addition to the above-mentioned protein-encoding genes, the losses of plastid tRNA genes (e.g., *trnV-UAC*, *trnG-UCC*, and *trnK-UUU*) were commonly observed in Santalales hemiparasites (Fig. 4). Previous studies have shown that some of the deleted tRNAs, such as *trnV-UAC*, are crucial for plastid translation and cell viability (Rogalski et al. 2008; Alkatib et al. 2012). Therefore, the reduction

of essential plastid tRNAs is a rare mutation in photosynthetic angiosperms. In addition to Santalales hemiparasites, it has so far only been observed in the Cactaceae subfamily Cactoideae (Morais et al. 2021). Nevertheless, Wicke and Naumann (2018) speculated that the import of tRNAs from the cytosol can be more easily achieved due to their relatively smaller size. Accordingly, it is expected that there should be a specific mechanism in photosynthetic plants that supplies the plastids with tRNAs from the cytosol (Morais et al. 2021). In view of the lack of empirical studies that determine the import of essential tRNAs into plastids in the literature (Rogalski et al. 2008; Alkatib et al. 2012; Morais et al. 2021), further investigations are needed to verify whether such tRNA import mechanisms exist in Santalales hemiparasites.

The phylogenetic relationships within Santalales reconstructed in this study based on the plastome data (Fig. 5) are highly consistent with those revealed by previous studies (Der and Nickrent 2008; Nickrent et al. 2010, 2019; Su et al. 2015; Chen et al. 2020a, b; Guo et al. 2020, 2021). The distribution of root and stem hemiparasites on the tree topologies suggested that stem hemiparasitism evolved at least twice from root parasitism in the sandalwood order. In addition to the family-specific loss or pseudogenization of plastid genes, the data also revealed that closely related taxa in the phylogenetic trees tended to possess high similarity in plastome size, structure, and gene content. This further supports the assumption that plastome degeneration in Santalales hemiparasites evolved in a lineage-specific manner (Chen et al. 2020a, b; Guo et al. 2020, 2021).

Does the endophytic habit lead to a higher level of plastome reduction in dwarf mistletoes?

Petersen et al. (2015) proposed that the variation in nutritional dependence on the host plant may influence the reductive evolution of plastomes in hemiparasites. Given that the endophytic habit indicates a greater reliance on host plants for nutrients and carbon requirement (Tocher et al. 1984; Kirkpatrick 1989; Singh and Carew 1989), it is expected to lead to a higher level of plastome reduction in dwarf mistletoes than other Santalales hemiparasites. A comparative analysis of plastome features between dwarf mistletoes and other Santalales hemiparasites provides good support for this assumption.

Overall, the *Arceuthobium* plastomes were distinctive among the examined Santalales hemiparasites in possessing the smallest size, lowest GC content, and relatively very few functional (intact) genes (Tables 2 and 3; Fig. 4). Compared with other Santalales hemiparasites, the deletion of all four RNA polymerase genes (*rpoA*, *rpoB*, *rpoC1*, and *rpoC2*) was a lineage-specific plastome mutation in *Arceuthobium*. The plastid *rpo* genes, which transcribe many plastid photosynthesis genes, are essential to all hemiparasites that retain their photosynthetic capacity (Wicke et al. 2013, 2016). In addition, the plastid *rpl33* gene, which encodes the ribosomal protein L33 (Rpl33), has been lost in all *Arceuthobium* species. Although *rpl33* is not essential for cell survival (Rogalski et al. 2008), the gene is rarely lost in angiosperms. To date, it has been merely known to be deleted from the plastomes of a few eudicot lineages, such as legume species (Fabaceae; Guo et al. 2007; Tangphatsornruang et al. 2010), Cactaceae subfamily Cactoideae (Morais et al. 2021), and mycoheterotrophic orchid *Rhizanthella* species (Wicke et al. 2011a,b). Remarkably, previous studies have revealed that the *rpl33* gene is indispensable for plants under stress conditions (Rogalski et al. 2008), because its function is particularly important for the formation of the photosynthetic apparatus at the young seedling stage and in young developing leaves (Fleischmann et al. 2011; Ehrnthaler et al. 2014). It is interesting to note that *Arceuthobium* species do not produce shoots immediately after seed germination but develop a highly developed endophytic system inside the branches of their host plants (Parmeter et al. 1959; Parmeter and Scharpf 1963; Tong and Ren 1980; Gilbert and Punter 1990, 1991). The endophytic system enables *Arceuthobium* species to absorb nutrition and water from host plants, making their survival at the young seedling stage completely independent of photosynthesis (Baranyay et al. 1971; Tocher et al. 1984; Alosi and Calvin 1985; Kirkpatrick 1989; Singh and Carew 1989). From this perspective, the endophytic habit of *Arceuthobium* species may largely relax the selection pressure to delete either *rpo* or *rpl33* genes from their plastomes. Collectively, it is reasonable to infer that the unique gene losses observed in *Arceuthobium* plastomes are likely correlated with the evolution of endophytic habit, which may have caused a higher level of plastome degradation in this genus.

Taxonomic implications

Arceuthobium is fairly unique among Santalales hemiparasites and possesses a remarkably host-specialized life history (Frank et al. 1996). On the other hand, *Arceuthobium* exhibits a high degree of morphological similarity across species, and species identification in the genus largely depends on the identity of their host plants (Frank et al. 1996; Qiu and Gilbert 2003). Therefore, it is difficult to reliably determine the identity of many herbarium specimens belonging to the genus whose host information is absent. Recently, DNA barcodes have been widely used to discriminate species (Hebert et al. 2003; Kress et al. 2005; Hollingsworth 2011; Hollingsworth et al. 2009, 2011, 2016). With the advent of next-generation sequencing technology, complete plastome sequences are increasingly used as extended DNA barcodes for species identification and discrimination (Coissac et al.

2016; Hollingsworth et al. 2016), especially in taxonomically perplexing plant taxa (e.g., Ruhsam et al. 2015; Firetti et al. 2017; Fu et al. 2019; Ji et al. 2019, 2020; Ślipiko et al. 2020). In this study, a high level of sequence divergence was detected among the plastomes of *A. chinense*, *A. pini*, and *A. sichuanense*, although these species have a fair degree of overlap in their morphological features and distribution ranges (Qiu and Gilbert 2003). This suggests that plastome sequencing may provide an effective solution for credibly identifying *Arceuthobium* specimens.

Conclusions

In this study, the plastomes of the dwarf mistletoes *Arceuthobium chinense* and *A. pini* were sequenced and assembled de novo. The newly generated plastomes were characterized by significant reductions in size and GC content, accompanied by the loss of several essential housekeeping genes (*rpoA*, *rpoB*, *rpoC1*, and *rpoC2*) and pseudogenization of some core photosynthetic genes (*psbZ* and *petL*). The results suggest that both the leafless and endophytic habitat of dwarf mistletoes may significantly relax the selection pressure on photosynthesis, as well as plastid transcription and translation, thus causing the loss/pseudogenization of such essential plastid-encoding genes. This implies that the higher level of plastome degradation in *Arceuthobium* species is likely correlated with the evolution of endophytic habit and highly reduced vegetative body. These findings provide new insights into the plastome reductive evolution associated with parasitism in Santalales and deepen our understanding of the biology of dwarf mistletoes.

Author contribution statement XG and YJ conceived and designed the research framework. GZ and LF collected sample; CL and XG collected and analyzed the data. XG and GZ wrote the original draft manuscript. YJ revised and edited the final manuscript. All authors have read and agreed to the published version of the manuscript.

Supplementary Information The online version contains supplementary material available at https://doi.org/10.1007/s00425-021-03643-y.

Acknowledgements This study was supported by the Second Tibetan Plateau Scientific Expedition and Research Program (2019QZKK04020103), and the National Natural Science Foundation of China (31060052). We are sincerely grateful to Prof. Wenhua Su for collecting sample of *Arceuthobium pini*, and to Lei Jin, Jin Yang, Naixing Shi, Li Li and Shuying Wang for their help in data analyses.

Data availability The newly sequenced plastomes in this study were deposited in the NCBI GenBank database under the accession number MT635188–MT635189 (Table 1).

Declarations

Conflict of interest The authors declare that the research was conducted in the absence of any commercial or financial relationships that could be construed as a potential conflict of interest.

.

References

Ahmed I, Biggs PJ, Matthews PJ, Collins LJ, Hendy MD, Lockhart PJ (2012) Mutational dynamics of aroid chloroplast genomes. Genome Biol Evol 4:1316–1323. https://doi.org/10.1016/bs.abr.2017.11.014

Alkatib S, Scharff LB, Rogalski M, Fleischmann TT, Matthes A, Seeger S, Schötler MA, Ruf S, Bock R (2012) The contributions of wobbling and superwobbling to the reading of the genetic code. PLoS Genet 8:e1003076. https://doi.org/10.1371/journal.pgen.1003076

Alosi MC, Calvin CL (1985) The ultrastructure of dwarf mistletoe *(Arceuthobium* spp.) sinker cells in the region of the host secondary vasculature. Can J Bot 63:889–898. https://doi.org/10.2307/2996548

Baranyay JA, Hawksworth FG, Smith RB (1971) Glossary of dwarf mistletoe terms. Canadian Forestry Service, Pacific Forest Research Centre, Victoria

Blazier JC, Guisinger-Bellian MM, Jansen RK (2011) Recent loss of plastidencoded *ndh* genes within *Erodium* (Geraniaceae). Plant Mol Biol 76:263–272. https://doi.org/10.1007/s11103-011-9753-5

Chang CC, Lin HC, Lin IP, Chow TY, Chen HH, Chen WH et al (2006) The chloroplast genome of *Phalaenopsis aphrodite* (Orchidaceae): Comparative analysis of evolutionary rate with that of grasses and its phylogenetic implications. Mol Biol Evol 23:279–291. https://doi.org/10.1093/molbev/msj029

Chen L, Yu R, Dai J, Liu Y, Zhou R (2020a) The loss of photosynthesis pathway and genomic locations of the lost plastid genes in a holoparasitic plant *Aeginetia indica*. BMC Plant Biol 20:199. https://doi.org/10.1186/s12870-020-02415-2

Chen XL, Fang DM, Wu CY, Liu B, Liu Y, Sahu SK et al (2020b) Comparative plastome analysis of root-and stem-feeding parasites of Santalales untangle the footprints of feeding mode and lifestyle transitions. Genome Biol Evol 12:3663–3676. https://doi.org/10.1093/gbe/evz271

Chumley TW, Palmer JD, Mower JP, Fourcade HM, Calie PJ, Boore JL et al (2006) The complete chloroplast genome sequence of *Pelargonium x hortorum*: organization and evolution of the largest and most highly rearranged chloroplast genome of land plants. Mol Biol Evol 23:2175–2190. https://doi.org/10.1093/molbev/msl089

Coissac E, Hollingsworth PM, Lavergne S, Taberlet P (2016) From barcodes to genomes: extending the concept of DNA barcoding. Mol Ecol 25:1423–1428. https://doi.org/10.1111/mec.13549

Daniel H, Lin CS, Yu M, Chang WJ (2016) Chloroplast genomes: diversity, evolution, and applications in genetic engineering. Genome Biol 17:134. https://doi.org/10.1186/s13059-016-1004-2

Der JP, Nickrent DL (2008) A molecular phylogeny of Santalaceae (Santalales). Syst Bot 33:107–116. https://doi.org/10.1600/036364408783887438

Dierckxsens N, Mardulyn P, Smits G (2017) NOVOPlasty: de novo assembly of organelle genomes from whole genome data. Nucleic Acids Res 45:e18. https://doi.org/10.1093/nar/gkw955

Doyle JJ, Doyle JL (1987) A rapid DNA isolation procedure for small quantities of fresh leaf tissue. Phytochem Bull 19:11–15

Ehrnthaler M, Scharff LB, Fleischmann TT, Hasse C, Ruf S, Bock R (2014) Synthetic lethality in the tobacco plastid ribosome and its rescue at elevated growth temperatures. Plan Cell 26:765–776. https://doi.org/10.1105/tpc.114.123240

Firetti F, Zuntini AR, Gaiarsa JW, Oliveira RS, Lohmann LG, Van Sluys MA (2017) Complete chloroplast genome sequences contribute to plant species delimitation: a case study of the *Anemopaegma* species complex. Am J Bot 104:1493–1509

Fleischmann TT, Scharff LB, Alkatib S, Hasdorf S, Schöttler MA, Bock R (2011) Nonessential plastid-encoded ribosomal proteins in tobacco: a developmental role for plastid translation and implications for reductive genome evolution. Plant Cell 23:3137–3155. https://doi.org/10.1105/tpc.111.088906

Frailey DC, Chaluvadi SR, Vaughn JN, Coatney CG, Bennetzen JL (2018) Gene loss and genome rearrangement in the plastids of five hemiparasites in the family Orobanchaceae. BMC Plant Biol 18:30. https://doi.org/10.1186/s12870-018-1249-x

Frank G, Hawksworth FG, Wiens D (1996) Dwarf mistletoes: biology, pathology, and systematics. United States Department of Agriculture Forest Service, Washington, DC

Fu CN, Wu CS, Ye LJ, Mo ZQ, Liu J, Chang YW et al (2019) Prevalence of isomeric plastomes and effectiveness of plastome superbarcodes in yews (*Taxus*) worldwide. Sci Rep-UK 9:2773. https://doi.org/10.1038/s41598-019-39161-x

Funk H, Berg S, Krupinska K, Maier U, Krause K (2007) Complete DNA sequences of the plastid genomes of two parasitic flowering plant species, *Cuscuta reflexa* and *Cuscuta gronovii*. BMC Plant Biol 7:45. https://doi.org/10.1186/1471-2229-7-45

Gilbert JA, Punter D (1990) Release and dispersal of pollen from dwarf mistletoe on jack pine in Manitoba in relation to microclimate. Can J for Res 20:267–273. https://doi.org/10.1139/x90-039

Gilbert JA, Punter D (1991) Germination of pollen of the dwarf mistletoe *Arceuthobium americanum*. Can J Bot 68:685–688. https://doi.org/10.1139/b91-092

Guo X, Ruan Z (2019a) Characterization of the complete plastome of *Dendrophthoe pentandra* (Loranthaceae), a stem hemiparasite. Mitochondr DNA B 4:3099–3100. https://doi.org/10.1080/23802359.2019.1667280

Guo X, Ruan Z (2019b) The complete chloroplast genome of *Elytranthe albida* (Loranthaceae), a hemiparasitic shru. Mitochondr DNA B 4:3112–3113. https://doi.org/10.1080/23802359.2019.1667911

Guo X, Castillo-Ramírez S, González V, Bustos P, Fernández-Vázquez JL, Santamaría RI, Arellano J, Cevallos MA, Dávila G (2007) Rapid evolutionary change of common bean (*Phaseolus vulgaris* L) plastome, and the genomic diversification of legume chloroplasts. BMC Genomics 8:228. https://doi.org/10.1186/1471-2164-8-228

Guo X, Ruan Z, Zhang G (2019) The complete plastome of *Taxillus vestitus* (Loranthaceae), a hemiparasitic plant. Mitochondr DNA B 4:3188–3189. https://doi.org/10.1080/23802359.2019.1667912

Guo X, Liu C, Zhang G, Su W, Landis JB, Zhang X et al (2020) The Complete plastomes of five hemiparasitic plants (*Osyris wightiana*, *Pyrularia edulis*, *Santalum album*, *Viscum liquidambaricolum*, and *V. ovalifolium*): comparative and evolutionary analyses within Santalales. Front Genet 11:597. https://doi.org/10.3389/fgene.2020.00597

Guo X, Liu C, Wang H, Zhang G, Yan H, Jin L, Su W, Ji Y (2021) The complete plastomes of two flowering epiparasites (*Phacellaria glomerata* and *P. compressa*): gene content, organization, and plastome degradation. Genomics 113:447–455. https://doi.org/10.1016/j.ygeno.2020.12.031

Hebert PDN, Cywinska A, Ball SL, De-Waard JR (2003) Biological identifications through DNA barcodes. Proc R Soc B 270:313–322. https://doi.org/10.1098/rspb.2002.2218

Hollingsworth PM (2011) Refining the DNA barcode for land plants. Proc Natl Acad Sci USA 108:19451–19452. https://doi.org/10.1073/pnas.1116812108

Hollingsworth PM, Forrest LL, Spouge JL, Hajibabaei M, Ratnasingham S, van der Bank M et al (2009) A DNA barcode for land plants. Proc Natl Acad Sci USA 106:12794–12797. https://doi.org/10.1073/pnas.0905845106

Hollingsworth PM, Graham SW, Little DP (2011) Choosing and using a plant DNA barcode. PLoS ONE 6:e19254. https://doi.org/10.1371/journal.pone.0019254

Hollingsworth PM, Li DZ, Michelle VDB, Twyford AD (2016) Telling plant species apart with DNA: from barcodes to genomes. Philos Trans R Soc B-Biol Sci 371:20150338. https://doi.org/10.1098/rstb.2015.0338

Horváth EM, Peter SO, Joë T, Rumeau D, Cournac L, Horváth GV, Kavanagh TA, Schäer C, Peltier G, Medgyesy P (2000) Targeted inactivation of the plastid *ndhB* gene in tobacco results in an enhanced sensitivity of photosynthesis to moderate stomatal closure. Plant Physiol 123:1337–1350. https://doi.org/10.1104/pp.123.4.1337

Hull RJ, Leonard OA (1964a) Physiological aspects of parasitism in mistletoes (*Arceuthobium* and *Phoradendron*). I. The carbohydrate nutrition of mistletoe. Am J Bot 39:996–1007. https://doi.org/10.1104/pp.39.6.996

Hull RJ, Leonard OA (1964b) Physiological aspects of parasitism in mistletoes (*Arceuthobium* and *Phoradendron*). II. The photosynthetic capacity of mistletoe. Am J Bot 39:1008–1017. https://doi.org/10.2307/4260344

Jansen RK, Cai Z, Raubeson LA, Daniell H, de Pamphilis CW, Leebens-Mack J et al (2007) Analysis of 81 genes from 64 plastid genomes resolves relationships in angiosperms and identifies genome–scale evolutionary patterns. Proc Natl Acad Sci USA 104:19369–19374

Ji Y, Liu C, Yang Z, Yang L, He Z, Wang H et al (2019) Testing and using complete plastomes and ribosomal DNA sequences as the next generation DNA barcodes in *Panax* (Araliaceae). Mol Ecol Resour 19:1333–1345. https://doi.org/10.1111/1755-0998.13050

Ji Y, Liu C, Yang J, Jin L, Yang Z, Yang JB (2020) Ultra-barcoding discovers a cryptic species in *Paris yunnanensis* (Melanthiaceae), a medicinally important plant. Front Plant Sci 11:411. https://doi.org/10.3389/fpls.2020.00411

Jiang D, Ma R, Li J, Mao Q, Miao N, Mao K (2019) Characterization of the complete chloroplast of *Scurrula parasitica*. Mitochondr DNA B 4:247–248. https://doi.org/10.1080/23802359.2018.1501294

Katoh K, Standley DM (2013) MAFFT multiple sequence alignment software version 7: improvements in performance and usability. Mol Biol 30:772–780. https://doi.org/10.1093/molbev/mst010

Kearse M, Richard M, Amy W, Steven SH, Matthew C, Shane S et al (2012) Geneious Basic: an integrated and extendable desktop software platform for the organization and analysis of sequence data. Bioinformatics 28:1647–1649. https://doi.org/10.1093/bioinformatics/bts199

Kirkpatrick LA (1989) Field study of water relations of dwarf mistletoe and lodgepole pine in central Oregon. Am J Bot 76:111–112

Krause K (2008) From chloroplasts to "cryptic" plastids: evolution of plastid genomes in parasitic plants. Curr Genet 54:111–121. https://doi.org/10.1007/s00294-008-0208-8

Kress WJ, Wurdack KJ, Zimmer EA et al (2005) Use of DNA barcodes to identify flowering plants. Proc Natl Acad Sci USA 102:8369–8374

Leonard OA, Hull RJ (1965) Translocation relationships in and between mistletoes and their hosts. Hilgardia 37:115–153. https://doi.org/10.3733/hilg.v37n04p115

Li Y, Zhou JG, Chen XL, Cui YX, Xu ZC, Li YH et al (2017) Gene losses and partial deletion of small single–copy regions of the chloroplast genomes of two hemiparasitic *Taxillus* species. Sci Rep 7:12834. https://doi.org/10.1038/s41598-017-13401-4

Lin CS, Chen JJ, Huang YT, Chan MT, Daniell H, Chang WJ et al (2015) The location and translocation of *ndh* genes of chloroplast origin in the Orchidaceae family. Sci Rep 5:9040. https://doi.org/10.1038/srep09040

Lin CS, Chen JJ, Chiu CC, Hsiao HC, Yang CJ, Jin XH et al (2017) Concomitant loss of NDH complex–related genes within chloroplast and nuclear genomes in some orchids. Plant J 90:994–1006. https://doi.org/10.1111/tpj.13525

Liu SS, Hu YH, Maghuly F, Porth IM, Mao JF (2018) The complete chloroplast genome sequence annotation for *Malania oleifera*, a critically endangered and important bioresource tree. Conserv Genet Res 11:271–274. https://doi.org/10.1007/s12686-018-1005-4

Liu X, Fu W, Tang Y, Zhang W, Song Z, Li L et al (2020) Diverse trajectories of plastome degradation in holoparasitic *Cistanche* and genomic location of the lost plastid genes. J Exp Bot 71:877–892. https://doi.org/10.1093/jxb/erz456

Maier UG, Krupinska K, Berg S, Funk HT, Krause K (2007) Complete DNA sequences of the plastid genomes of two parasitic flowering plant species, *Cuscuta reflexa* and *Cuscuta gronovii*. BMC Plant Biol 7:1–12. https://doi.org/10.1186/1471-2229-7-45

Mathiasen LM, Shaw DC, Nickrent DL, Watson DM (2008) Mistletoes: pathology, systematics, ecology, and management. Plant Dis 92:988–1006. https://doi.org/10.1094/PDIS-92-7-0988

Mayor C, Brudno M, Schwartz JR, Poliakov A, Rubin EM, Frazer KA, Pachter LS, Dubchak I (2000) VISTA: visualizing global DNA sequence alignments of arbitrary length. Bioinformatics 16:1046–1047

McCoy SR, Kuehl JV, Boore JL, Raubeson LA (2008) The complete plastid genome sequence of *Welwitschia mirabilis*: an unusually compact plastome with accelerated divergence rates. BMC Evol Biol 8:130. https://doi.org/10.1186/1471-2148-8-130

McNeal JR, Kuehl JV, Boore JL, Pamphilis CWD (2007) Complete plastid genome sequences suggest strong selection for retention of photosynthetic genes in the parasitic plant genus *Cuscuta*. BMC Plant Biol 7:57. https://doi.org/10.1186/1471-2229-7-57

Millen RS, Olmstead RG, Adams KL et al (2001) Many parallel losses of *infA* from chloroplast DNA during angiosperm evolution with multiple independent transfers to the nucleus. Plant Cell 13:645–658. https://doi.org/10.3732/ajb.0800085

Morais SG, Lopes AS, Gomes PT et al (2021) Genetic and evolutionary analyses of plastomes of the subfamily Cactoideae (Cactaceae) indicate relaxed protein biosynthesis and tRNA import from cytosol. Braz J Bot 44:97–116. https://doi.org/10.1007/s40415-020-00689-2

Neuhaus HE, Emes MJ (2000) Nonphotosynthetic metabolism in plastids. Annu Rev Plant Physiol Plant Mol Biol 51:111–140. https://doi.org/10.1146/annurev.arplant.51.1.111

Ni Z, Ye Y, Bai T, Xu M, Xu LA (2017) Complete chloroplast genome of *Pinus massoniana* (Pinaceae): gene rearrangements, loss of ndh Genes, and short inverted repeats contraction. Expansion Mol 22:1528. https://doi.org/10.3390/molecules22091528

Nickrent DL (1997) The parasitic plant connection. Available online: http://parasiticplants.siu.edu/. Accessed 7 September 2019

Nickrent DL (2002) Plantas parásitas en el mundo. In: López-Sáez JA, Catalán P, Sáez L (eds) Plantas Parásitas de la Península Ibérica e Islas Baleares. Mundi-Prensa Libros, Madrid, pp 7–27

Nickrent DL, Malécot V, Vidal-Russell R, Der JP (2010) A revised classification of Santalales. Taxon 59:538–558. https://doi.org/10.2307/25677612

Nickrent DL, Anderson F, Kuijt J (2019) Inflorescence evolution in Santalales: integrating morphological characters and molecular phylogenetics. Am J Bot 106:402–414. https://doi.org/10.1002/ajb2.1250

Palmer JD (1985) Comparative organization of chloroplast genomes. Ann Rev Genet 19:325–354. https://doi.org/10.1146/annurev.ge.19.120185.001545

Park S, Jansen RK, Park S (2015) Complete plastome sequence of Thalictrum coreanum (Ranunculaceae) and transfer of the rpl32 gene to the nucleus in the ancestor of the subfamily Thalictroideae. BMC Plant Biol 15:40. https://doi.org/10.1186/s12870-015-0432-6

Parks CG, Flanagan PT (2001) Dwarf mistletoes (*Arceuthobium* spp.), rust diseases, and stem decays in eastern Oregon and Washington. Northwest Sci 75:31–337. https://doi.org/10.2307/3858451

Parmeter JR, Scharpf RF (1963) Dwarf mistletoe on red fir and white fir in California. J Forest 61:371–374. https://doi.org/10.1093/jof/61.5.371

Parmeter JR, Hood JR, Scharpf RF (1959) *Colletotrichum* blight of dwarf mistletoe. Phytopathol 49:812–815

Pel HJ, Grivell LA (1994) Protein synthesis in mitochondria. Mol Biol Rep 165:183–194

Peredo EL, King UM, Les DH (2013) The plastid genome of *Najas flexilis*: adaptation to submersed environments is accompanied by the complete loss of the NDH complex in an aquatic angiosperm. PLoS ONE 8:e68591. https://doi.org/10.1371/journal.pone.0068591

Petersen G, Cuenca A, Seberg O (2015) Plastome evolution in hemiparasitic mistletoes. Genome Biol Evol 7:2520–2532. https://doi.org/10.1093/gbe/evv165

Qiu HX, Gilbert MG (2003) Viscaceae. In *Flora of China*, Vol. 5; Z. Y. Wu, P. H. Raven (Eds), pp. 241–242. Beijing, Science Press; aint Louis, Missouri Botanical Garden Press.

Rogalski M, Karcher D, Bock R (2008) Superwobbling facilitates translation with reduced tRNA sets. Nat Struct Mol Biol 15:192–198. https://doi.org/10.1038/nsmb.1370

Ronquist F, Huelsenbeck JP (2003) MrBayes 3: Bayesian phylogenetic inference under mixed models. Bioinformatics 19:572–1574. https://doi.org/10.1093/bioinformatics/btg180

Ruhsam M, Rai HS, Mathews S, Ross G, Graham SW, Raubeson LA et al (2015) Does complete plastid genome sequencing improve species discrimination and phylogenetic resolution in *Araucaria*? Mol Ecol Resour 15:1067–1078. https://doi.org/10.1111/1755-0998.12375

Rumeau D, Peltier G, Cournac L (2007) Chlororespiration and cyclic electron flow around PSI during photosynthesis and plant stress response. Plant Cell Environ 30:1041–1051. https://doi.org/10.1111/j.1365-3040.2007.01675.x

Sabir J, Schwarz EN, Ellison N, Zhang J, Baeshen NA, Mutwakil M, Jansen RK, Ruhlman TA (2014) Evolutionary and biotechnology implications of plastid genome variation in the inverted–repeat lacking clade of legumes. Plant Biotechnol J 12:743–754

Sanderson MJ, Copetti D, Búrquez A, Bustamante E, Charboneau JLM, Eguiarte LE et al (2015) Exceptional reduction of the plastid genome of saguaro cactus (*Carnegiea gigantea*): loss of the *ndh* gene suite and inverted repeat. Am J Bot 102:1115–1127. https://doi.org/10.3732/ajb.1500184

Saski C, Lee S-B, Daniell H, Wood TC, Tomkins J, Kim H-G, Jansen RK (2005) Complete chloroplast genome sequence of *Glycine max* and comparative analyses with other legume genomes. Plant Mol Biol 59:309–322

Schattner P, Brooks AN, Lowe TM (2005) The tRNAscan-SE, snoscan and snoGPS web servers for the detection of tRNAs and snoRNAs. Nucleic Acids Res 33:W686–W689. https://doi.org/10.1093/nar/gki366

Schneider AC, Chun H, Stefanović S, Baldwin BG (2018) Punctuated plastome reduction and host–parasite horizontal gene

transfer in the holoparasitic plant genus *Aphyllon*. Proc R Soc B 285:20181535. https://doi.org/10.1098/rspb.2018.1535
Schwarz EN, Ruhlman TA, Sabir JS, Hajrah NH, Alharbi NS, Al-Malki AL et al (2015) Plastid genome sequences of legumes reveal parallel inversions and multiple losses of *rps16* in papilionoids. J System Evol 53:458–468
Shin HW, Lee NS (2018) Understanding plastome evolution in hemiparasitic Santalales: complete chloroplast genomes of three species, *Dendrotrophe varians, Helixanthera parasitica,* and *Macrosolen cochinchinensis*. PLoS ONE 13:e0200293. https://doi.org/10.1371/journal.pone.0200293
Singh P, Carew GE (1989) Impact of eastern dwarf mistletoe in black spruce forests in Newfoundland. Eur J for Pathol 19:305–322. https://doi.org/10.1111/j.1439-0329.1989.tb00266.x
Ślipiko M et al (2020) Molecular delimitation of European leafy liverworts of the genus Calypogeia based on plastid superbarcodes. BMC Plant Biol 20:243. https://doi.org/10.1186/s12870-020-02435-y
Stamatakis A, Hoover P, Rougemont J (2008) A rapid bootstrap algorithm for the RAxML web servers. Syst Biol 57:758–771. https://doi.org/10.1080/10635150802429642
Straub SCK, Parks M, Weitemier K, Fishbein M, Cronn RC, Liston A (2012) Navigating the tip of the genomic iceberg: next-generation sequencing for plant systematics. Am J Bot 99:349–364. https://doi.org/10.3732/ajb.1100335
Su HJ, Hu JM (2016) The complete chloroplast genome of hemiparasitic flowering plant *Schoepfia jasminodora*. Mitochondr DNA B 1:767–769. https://doi.org/10.1080/23802359.2016.1238753
Su HJ, Hu JM, Anderson FE, Nickrent DL (2015) Phylogenetic relationships of Santalales with insights into the origins of holoparasitic Balanophoraceae. Taxon 64:491–506. https://doi.org/10.12705/643.2
Sun Y, Moore MJ, Zhang S, Soltis PS, Soltis DE, Zhao T et al (2016) Phylogenomic and structural analyses of 18 complete plastomes across nearly all families of early–diverging eudicots, including an angiosperm wide analysis of IR gene content evolution. Mol Phylogenet Evol 96:93–101. https://doi.org/10.1016/j.ympev.2015.12.006
Sun Y, Moore MJ, Lin N, Adelalu KF, Meng A, Jian S et al (2017) Complete plastome sequencing of both living species of Circaeasteraceae (Ranunculales) reveals unusual rearrangements and the loss of the *ndh* gene family. BMC Genomics 18:592. https://doi.org/10.1186/s12864-017-3956-3
Tangphatsornruang S, Sangsrakru D, Chanprasert J, Uthaipaisanwong P, Yoocha T, Jomchai N, Tragoonrung S (2010) The chloroplast genome sequence of mungbean (*Vigna radiata*) determined by high-throughput pyrosequencing: structural organization and phylogenetic relationships. DNA Res 17:11–22. https://doi.org/10.1093/dnares/dsp025
Tocher RD, Gustafson SW, Knutson DM (1984) Water metabolism and seedling photosynthesis in dwarf mistletoes. In: Hawksworth FG, Scharpf F (eds) Biology of dwarf mistletoes, Proceedings of the symposium. Department of Agriculture, Forest Service, Fort Collins, pp 62–69
Tong J, Ren W (1980) Preliminary studies on the disease cycle of *Arceuthobium chinense*. J Yunnan for Coll 1:19–25
Wakasugi T, Tsudzuki J, Ito S, Nakashima K, Tsudzuki T, Sugiur M (1994) Loss of all *ndh* genes as determined by sequencing the entire chloroplast genome of the black pine *Pinus thunbergii*. Proc Natl Acad Sci USA 91:9794–9798. https://doi.org/10.2307/2365708
Wicke S, Naumann J (2018) Molecular evolution of plastid genomes in parasitic flowering plants. Adv Bot Res 85:315–347. https://doi.org/10.1016/bs.abr.2017.11.014
Wicke S, Schneeweiss GM, de Pamphilis CW, Müller KF, Quandt D (2011a) The evolution of the plastid chromosome in land plants: gene content, gene order, gene function. Plant Mol Biol 76:273–297
Wicke S, Schneeweiss GM, Depamphilis CW, Kai FM, Quandt D (2011b) The evolution of the plastid chromosome in land plants: gene content, gene order, gene function. Plant Mol Biol 76:273–297. https://doi.org/10.1007/s11103-011-9762-4
Wicke S, Müller KF, Depamphilis CW, Quandt D, Wickett NJ, Zhang Y et al (2013) Mechanisms of functional and physical genome reduction in photosynthetic and nonphotosynthetic parasitic plants of the broomrape family. Plant Cell 25:3711–3725. https://doi.org/10.1105/tpc.113.113373
Wicke S, Müller KF, Depamphilis CW, Quandt D, Bellot S, Schneeweiss GM (2016) Mechanistic model of evolutionary rate variation en route to a nonphotosynthetic lifestyle in plants. Proc Natl Acad Sci USA 113:9045–9050. https://doi.org/10.1073/pnas.1607576113
Wu CS, Lai YT, Lin CP, Wang YN, Chaw SM (2009) Evolution of reduced and compact chloroplast genomes (cpDNAs) in gnetophytes: selection toward a lower–cost strategy. Mol Phylogenet Evol 52:115–124. https://doi.org/10.1016/j.ympev.2008.12.026
Wyman SK, Jansen RK, Boore JL (2004) Automatic annotation of organellar genomes with DOGMA. Bioinformatics 20:3252–3255. https://doi.org/10.1093/bioinformatics/bth352
Yang GS, Wang YH, Shen SK (2017) The complete chloroplast genome of a vulnerable species *Champereia manillana* (Opiliaceae). Conserv Genet Resour 3:415–418. https://doi.org/10.1007/s12686-017-0697-1
You M (1985) The study of the physiological and biochemical characteristics on the parasitic disease by *Arceuthobium chinense* Lecomte. J Southwest for Coll 6:8–16
You M, Tong J (1987) Study on biology of Arceuthobium chinense and its harm set to *Keteleeria evelyniana*. J Southwest for Coll 7:38–46
Yu NJ, Spremulli LL (1998) Regulation of the activity of chloroplast translational initiation factor 3 by NH_2- and COOH-terminal extensions. J Biol Chem 165:3871–3877
Zhu ZX, Wang JH, Cai YC, Zhao KK, Moore MJ, Wang HF (2018) Complete plastome sequence of *Erythropalum scandens* (Erythropalaceae), an edible and medicinally important liana in China. Mitochondr DNA B 3:139–140. https://doi.org/10.1080/23802359.2017.1413435